Meteorol. Atmos. Phys. 56, 33–55 (1995)

Meteorology and Atmospheric Physics

Program in Atmospheric and Oceanic Sciences, University of Colorado, Boulder, Colorado, U.S.A.

The Annual Cycle and the Predictability of the Tropical Coupled Ocean-Atmosphere System

P. J. Webster

With 18 Figures

Received February 21, 1994

Summary

Using large-scale circulation statistics from the Pacific Ocean basin, predictability of the coupled ocean-atmosphere system on interannual time scales is found both to be limited in extent and to possess a strong annual cycle. Irrespective of when lagged correlations are commenced, correlations decrease rapidly through the boreal spring, indicating an inherent predictability limitation for large scale coupled oceanic-atmospheric processes such as El Niño. Long term prediction experiments using numerical coupled-models show that the models are excellent facsimiles of the real system. They, too, encounter the predictability barrier and exhibit a substantial decrease in observation-prediction correlation across the boreal spring. Thus, a predictive system based solely on the interactive physics of the Pacific Basin appears limited to a maximum of less than one year and a minimum of only one or two months.

Two hypotheses are made to explain the existence of the predictability barrier. First, it is argued that the tropical coupled system is at its frailest state during the boreal spring and that the signal-to-noise ratio is weakest. In such a system, maximum random error growth may occur as the atmosphere and the ocean become temporally detached and wander onto different climate trajectories. A series of 144 preliminary Monte Carlo experiments were conducted with a coupled ocean-atmosphere model to test the hypothesis. Irrespective of when the experiments were commenced, error growth was maximized at the same time of the year. The second hypothesis suggests that the near-equatorial circulation is perturbed at the time of its weakest state by external influences such as the monsoon and that the climate wanderings are "nudged" deterministically. There is observational and theoretical evidence to support the hypothesis. Observations suggest that anomalous monsoons impart basin-wide coherent alterations of the wind stress field in the Pacific Ocean. Experiments with a coupled ocean-atmosphere model show that the period of an ENSO event is altered substantially by an anomalous monsoon. Given that there appear to be precursors to anomalous monsoons, it is suggested that there may be ways to avoid the predictability barrier and thus extend prediction of the entire system.

Finally, noting that the two hypotheses are not mutually exclusive, they are combined to form a unified theory. As the asymmetric monsoonal and the symmetric near-equatorial heating are in approximate quadrature, it is argued that the monsoons influence the Walker circulation during the boreal spring. However, during the boreal fall and early winter the near-equatorial heating variability dominates the winter monsoon.

1. Introduction

During the last century considerable attention has been given to the forecasting or "foreshadowing" of large scale climatic variations. For example, Walker (1923, 1924) sought precursors of the Indian monsoon system and uncovered a labyrinth of low frequency circulation systems that spanned vast reaches of the globe. Of singular importance was the Southern Oscillation (SO), a "swaying" with a time scale of 3–5 years that produces an out-of-phase relationship in surface pressure between the eastern and western hemispheres (Walker, 1923, 1924; Troup, 1965). However, rather finding precursors of the monsoon from the year-to-year variability of the SO, a contrary view emerged:

"... *Unfortunately for India, the SO in June-August, at the height of the monsoon, has many significant correlations with later events and relatively few with earlier events... The Indian monsoon therefore stands out as an active, not a passive feature in world weather, more efficient as a broadcasting tool rather than an event to be forecast. Overall, Walker's worldwide survey ended offering promise for the prediction of events in other regions rather than in India...*" (Normand, 1953).

Thus, the pioneers in the study of the low-frequency climate variability recognized at an early time that there was a distinct sequential relationship between the monsoon and SO. That is, variations in the monsoon probably lead variations in the basic rhythm of the SO and, hence, the El Niño phenomena itself.

It is important to understand the significance of these early findings. No other major atmospheric circulation system appears to lead the El Niño-Southern Oscillation phenomenon (ENSO) in the manner of the Asian-Australasian monsoon system. The magnitude and phase of ENSO may be sensitive to other factors that influence the ocean structure but the monsoon is a circulation feature that is planetary in scale and possesses an identifiable signal regarding its subsequent intensity some nine months prior to the active stage of the summer monsoon (Webster and Yang, 1992; Vernekar et al., 1994). Furthermore, the magnitude of the variability of the monsoon is substantial and identifiable over a large area including the Pacific Ocean basin (Webster and Yang, 1992).

Bjerknes (1969) provided a physical context for the statistical work of Walker by suggesting a role for the oceans (specifically the Pacific Ocean) in the SO. In his context, the SO was related to the aperiodic El Niño migrations in the near-equatorial sea-surface temperature (SST). From this relationship grew the concept of El Niño-Southern oscillation or ENSO. Bjerknes extended the equatorial context of ENSO by noting corresponding high latitude circulation changes. He referred to those remote geographical connections as "teleconnections". Subsequent theoretical work led to a description and numerical modelling of the evolving coupled ocean-atmosphere system in the Pacific Ocean (see Philander, 1990). With this modelling capability, the prospect of interannual prediction appeared possible. If the El Niño phenomena could be forecast, then, by extension, the variations of global-climate through Bjerknes' teleconnection relationships, could also be foreshadowed. In fact, the first part of the problem, the forecasting of the coupled state in the Pacific Ocean, has been undertaken with moderate success (e.g., Cane, 1991; Cane and Zebiak, 1985; Zebiak and Cane, 1987; Latif and Graham, 1991; among others).

Modeling and predicting the coupled ocean-atmosphere system takes advantage of the fact that there are two major time scales in oceanic dynamics. The first time-scale depends on the local influence on the ocean of surface buoyancy fluxes and wind stress into the ocean from the atmosphere. These processes may be generally referred to as thermodynamical and dynamical forcing of the ocean, respectively. The second time scale is determined by the intrinsic dynamical response of the ocean to the rectified thermodynamical and dynamical forcing. This response is manifested in the form of planetary waves. Whether or not the ocean will respond to the local forcing and produce a rectified lower frequency dynamic response depends on the relative frequency of the atmospheric forcing (ω_{atm}) and the intrinsic frequency of ocean dynamics (ω_{oce}).

In the extratropics, the local forcing of the ocean by wind stress is very strong at frequencies associated with transient atmospheric disturbances. These frequencies are very high compared to oceanic dynamical time scales. The latter are determined, principally, by the local geostrophic adjustment time scale of the ocean and the speed of the ensuing wave propagation. Each of these scales is extremely slow compared to the time scales of atmospheric forcing of the ocean. For example, an extratropical ocean Rossby wave would take about a decade to propagate across an ocean basin. That is, $\omega_{atm} \gg \omega_{oce}$. Thus, in general, atmospheric stochastic forcing dominates and the extratropical ocean remains in near thermodynamical equilibrium with the atmospheric forcing. At the same time, the stochastic forcing renders the extratropical coupled system into a state of perpetual dynamical imbalance.

The amplitude of stochastic atmospheric forcing over much of the tropical oceans is relatively small compared to the extratropics. However, in the very narrow region about the equator, referred to as the equatorial wave guide, equatorially trapped

waves propagate rapidly from one side of an ocean basin to the other. Kelvin waves cross the Pacific basin in less than two months. The return passage of the impulse, in the form of a reflected Rossby wave packet takes longer than a year. Thus, in the tropics, the dynamic time scale is sufficiently rapid and the stochastic forcing of sufficiently small amplitude that a dynamic ocean signal can pass from one side of the ocean basin to the other without being obliterated by atmospheric noise. That is, $\omega_{atm} \approx \omega_{oce}$. As distinct from higher latitudes, basin-wide *oceanic* teleconnections are possible at low latitude. In the extratropics, teleconnections are predominantly atmospheric. Figure 1 shows a schematic of the different time scales and processes in the extratropics and the tropics. The diagram shows the response of the ocean to impulsive atmospheric forcing occurring in the high latitudes (left panel) and the equatorial regions (right panel) and the combined coupled system response.

A central aim of the ten-year (1985–1994) Tropical Ocean-Global Atmosphere (TOGA) Program (WCRP 1986) was to gather data for the development and testing of the ENSO hypotheses and to build upon empirical forecasting endeavors such as those developed by Nicholls (1984). The scientific objectives of TOGA centered around the description and prediction of coupled ocean-atmosphere variability. TOGA provided a major incentive for the development of coupled ocean-atmosphere models that would emulate ENSO processes. Figure 2 shows the generic structure of models constructed to simulate ENSO and to test its predictability. The model system usually contains a global atmosphere which is normally steady state and free-surface (and thus divergent) of the Gill-type (Gill, 1980) coupled to a global ocean. The atmosphere drives rapid dynamic modes primarily in the equatorial wave guide through wind stress. In turn, the ocean drives the atmosphere by heat fluxes associated with the anomalies in the predicted SST. Such coupled ocean-atmosphere surrogates will be referred to as "ENSO-models".

The separation of the equatorial and extratropical oceans into different dynamic regimes is probably an oversimplification. The geotrophic adjustment time scales and the Rossby wave propagation and group speeds decrease with latitude rather smoothly. Thus, it is possible that the oceanic dynamics in the subtropics may play non-inconsequential roles in interannual variability.

Despite the moderate success in simulating and predicting ENSO, there are still a number of theories of why ENSO occurs at all (see, e.g., Philander, 1990; Neelin, 1991; Neelin and Jin, 1993; Hao et al., 1993). Most theoretical explanations center around the concept of the delayed oscillator in which successive reflections of oceanic planetary waves within the ocean basins determine an intrinsic

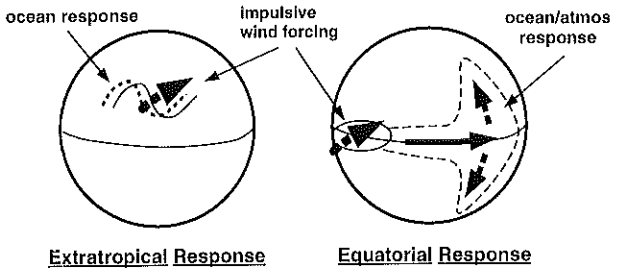

Fig. 1. The basic difference between the response of the extratropical and the near equatorial oceans to impulsive forcing. In the equatorial regions, the dynamic response time of the ocean is very rapid and similar in time scale to the variability of the atmospheric forcing. Towards higher latitudes, the dynamic propagation of ocean response becomes much slower than the atmospheric forcing variability. Thus, near the equator, waves may propagate from one side of the basin to the other in a combined mode with the atmosphere to form a dynamic coupled teleconnections. At higher latitudes, the higher frequency forcing destroys the oceanic dynamic signal very rapidly. There, teleconnections are principally atmospheric

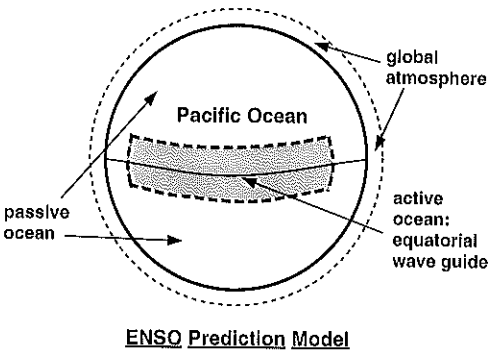

Fig. 2. The basic structure of intermediate complexity coupled ocean-atmosphere models used to simulate and predict ENSO variations in the Pacific Ocean basin. The ocean is, effectively, a dynamic strip in the Pacific Ocean surrounded by an ocean that is continually adjusting to white noise forcing by the atmophere. The ocean is surmounted by a global atmosphere assumed to be in perpetual steady state relative to the evolving ocean

time scale for interannaul variability (Battisti and Hirst, 1989). Battisti and Hirst also address why ENSO-like phenomena appear to be restricted to the Pacific Ocean basin. They argue that for basin sizes less than 13,000 km, thus excluding the Indian and the Atlantic oceans, interannual variability of the type endemic to the Pacific cannot be present. This is because, according to the delayed oscillator theory, the translation time scales of the reflected mode packets necessary for interannual variability in the Pacific Ocean, have too rapid trans-basin propagations. At the same time, the location of the background warm pools about the Indonesian Archipelago would seem to be important in acting as a restoring factor in the delayed oscillator. The physical processes that create the background SST distribution are discussed by Webster (1994).

However, there is still some uncertainty about whether the Atlantic ocean does undergo El Niño-like oscillations. During 1984, for example, the year following the major warming event in the Pacific Ocean, an El Niño-like event occurred in the Atlantic. Whether or not the event was an intrinsic coupled ocean-atmosphere property of the Atlantic or whether it resulted from adjustment of the tropical atmosphere following the major Pacific event, and was, thus, a forced response, is not known. Besides the Battisti-Hirst scaling criterion, there are probably two other reasons that the El Niño-like oscillations have not occurred in the Indian Ocean. First, the strong annual cycle creates wave packets that probably obliterate an interannual signal. Second, the thermocline in the Indian Ocean shoals to the west. Thus an eastward propagating and downwelling Kelvin wave would keep warm water restricted to the eastern Indian Ocean.

In this note, the degree to which interannual variability can be predicted, at least within the confines of the ENSO model structure, will be discussed. It will be shown that although there have been sound strides towards attaining the objectives of the TOGA experiment, there are distinct limits to the predictability of the coupled ocean-atmosphere system using ENSO-type models. Specifically, models appear to lose predictability during the boreal spring period with limits that are very similar to those hinted at in diagnostic studies of the observed coupled system. The central aim of this study will be to identify whether or not these limits suggest that there is an inherent limit to interannual predictability, or whether the ENSO modelling system is too simple to simulate longer period predictability that may exist in the real system.

In Section 2, it is shown that model depletions of predictability mirror the lagged correlations of observed ENSO indices. The third Section shows examples of coupled system predictions. The strong relationship between the ENSO phenomena and the annual cycle is discussed in Section 4. Two hypotheses that may explain why there is a predictability barrier are posited in Section 5. Sections 6 and 7 show modelling studies aimed at testing the hypotheses. The results are summarized in Section 8 and a unified hypothesis is proposed.

2. Observed ENSO Correlations

A measure of Walker's SO is the normalized surface pressure difference between Tahiti and Darwin. This is referred to as the Southern Oscillation Index (SOI) which also provides a rough measure of the strength of the equatorial Walker Circulation (Webster, 1983). It is simple to compute and can be reconstructed as a more or less continuous series for over 100 years. Major negative periods of the SOI corresponds to El Niño or warm Pacific Ocean events while positive periods of SOI correspond to La Niña or cold events. Warm events appear aperiodically every 3 to 5 years. Recent studies (e.g., Yasunari, 1987, 1991; Rasmusson et al., 1990) suggest that there is also a biennial component to SOI variability.

To compute the SOI (see, e.g., Trenberth, 1984), the annual cycle is removed from the pressure difference time series to provide a simple measure of interannual variability. However, while the interannual variability is elucidated by this subtraction, some important features of the climate system may be masked. Troup (1965) shows that the spatial distribution of interannual variability possesses a distinct annual cycle. For example, extrema of surface pressure for a specific value of the SOI were shown to move by 90 degrees of longitude from summer to winter.

Figure 3a shows the lagged correlations of the mean monthly values of the SOI (Webster and Yang, 1992). The lagged correlations provide information about the relationship of elements in a series with subsequent or previous values. The

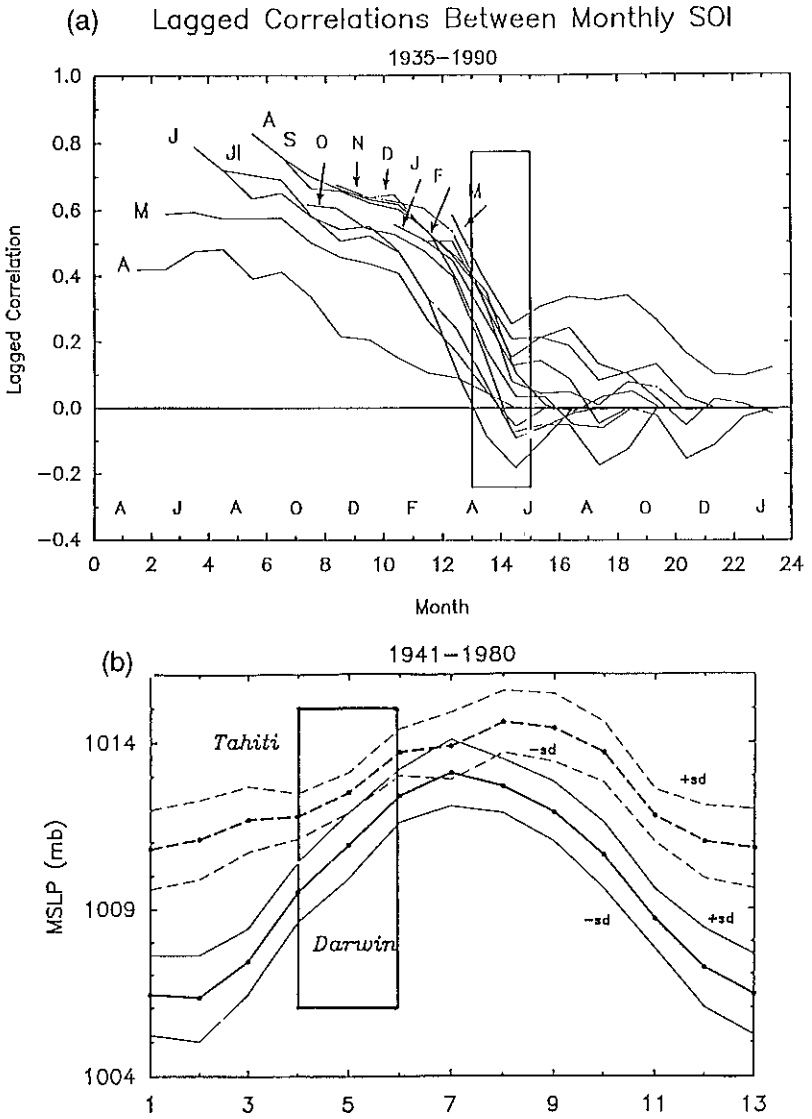

Fig. 3. (a) Lagged correlations between the mean monthly Southern Oscillation Index (SOI). Letters indicate the anchor or starting month of the correlation. The plot is offset so that the correlations of the same month are lined up along the abscissa. The box indicates the boreal spring period. (b) The long-term average annual cycle of the Darwin (solid lines) and the Tahiti mean sea level pressure (dashed). The difference of these two pressure traces is normally subtracted out from the record when the SOI is computed (Webster and Yang, 1992)

analysis here shows lagged correlations of the SOI commencing at different starting months. The curves are offset so that the correlations for the same month are lined up along the abscissa. With this reorientation a remarkable feature emerges. Irrespective of the time of year when lagged correlations are commenced, a rapid decrease occurs across the boreal spring. The period of correlation demise (March-May) is enclosed within the box. A similar decrease is absent during the boreal autumn.

There are a number of consequences that arise from the one-sided SOI correlation distribution. For example, a knowledge of the history of the SOI in June will allow the SOI to be foreshadowed until the following spring, or over a period of 10 months. However, a knowledge of the SOI in February or March does not provide any information regarding the SOI beyond a month or two. Thus, the boreal spring appears to be a "correlation barrier", at least as far as the SOI is concerned. Furthermore, if the SOI is correlated simultaneously with the strength of the monsoon (i.e., a negative SOI is often associated with a weak monsoon; Rasmusson and Carpenter, 1983; Shukla, 1987a, b), a correlation demise during the boreal spring means that the previous values of the SOI for as late as spring cannot provide any significant information about the strength of the summer monsoon. Thus, a foreshadowing of the summer monsoon by ENSO statistics is limited to only a month or two prior to the onset of the summer monsoon. On the other hand, the winter monsoon can be foreshadowed by a knowledge of the SOI

some 6–8 months previously. As the boreal winter values of the SOI correlate strongly with the strength of the winter monsoon, the strong lag correlation suggests meaningful prediction of the winter monsoon.

The decrease in the SOI lagged correlations at a particular time of year indicates that the annual cycle appears as a major influence in ENSO physics. The annual cycle of the SOI, normally extracted from the index, is shown in Fig. 3b and depicts the strength of the pressure gradient along the equator or the strength of the along-equator flow or, alternatively, the annual cycle of the intensity of the Walker Circulation. The figure shows clearly that at the time of the correlation decrease the zonal pressure gradient, and hence, the along-equator flow, is weakest. At this same time, the western Pacific Ocean is undergoing rapid reorientations of its heat source and sink distribution and the Asian summer monsoon system is starting to accelerate. Thus, simultaneously, the along-equatorial flow approaching its weakest state whilst the off-equator circulations are starting to approach their strongest.

3. ENSO Model Simulations and Predictability

The utility of ENSO-type coupled ocean-atmosphere models (Fig. 2) in simulating the structure of ENSO has been demonstrated with extended integrations (see, Cane, 1991; for review). The character of the interannual variability from these very long runs appears quite similar to the observational record. With a modest degree of success,

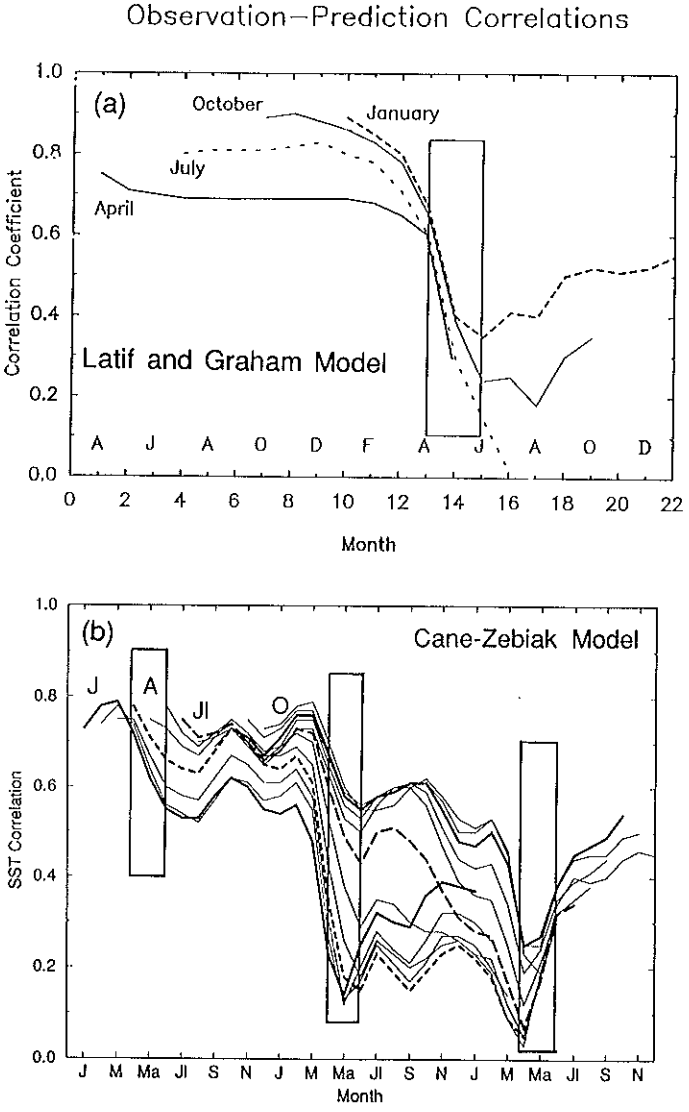

Fig. 4. The correlations between the SST predictions of coupled ocean atmosphere models and observations of the Pacific Ocean SST using the same format as Fig. 3. The models are: (a) The Latif-Graham model, and (b) the Cane-Zebiak model. Boxed region indicates the boreal spring. Notice that there is a significant correlation decrease at the same time of year in both models. Note, too, the similarity of the model results with the SOI lagged correlations shown in Fig. 3a

the simulation capability has been translated into prediction, at least in the Pacific Ocean region.

The extent to which the models are successful in simulation can be quantified by comparing the forecast fields with observations. Examples of model prediction-observation correlations are shown in Fig. 4a and b for two forecast models: the Latif-Graham model (Latif and Graham, 1991) and the Cane-Zebiak model (Cane and Zebiak: personal communication). The analysis of the Latif-Graham model is based on one year of integrations and comparison. The Cane-Zebiak correlations, on the other hand, are based on a much longer record. Using the comparative method deployed in Fig. 3b, the forecast-observation correlations are offset in order to compare the skill of the forecasts for the same month. In each model, the forecast skill decreases very rapidly across the boreal spring. Because of the much longer record, successive decreases can be seen in each spring in the Cane-Zebiak model. Following the first spring, there is a slight increase of predictability. This characteristic can also be seen from the Latif-Graham study. However, the most important characteristic of both models is an uneven cascase of forecast skill with major reductions occurring across the boreal spring.

An important point to note is that the two models discussed here are completely different. The Latif-Graham model is a hybrid statistical-dynamical model. The Cane-Zebiak model, on the other hand, is an "anomaly" coupled ocean atmospheric model very similar to the ENSO-type model shown in Fig. 1. An anomaly model considers quantities which are differences (or anomalies) from a prescribed annual cycle.

Perhaps the most important deduction that can be made from Fig. 4 is that two very different models appear to be behaving very similarly to the SOI correlations shown in Fig. 3a. The similarity of the observed structure of the coupled ocean-atmosphere system and model simulations raises a number of important questions:

(i) What is the role of the annual cycle in the ENSO process? Given that the correlation decrease in both observations and models appear to occur at the same time of the year, it would seem that some aspect of the annual cycle is an important component of the predictability puzzle.

(ii) Why is the correlation demise one-sided? Why doesn't a similar decrease occur at the autumnal equinox?

(iii) Are both the models and observations indicating an inherent limitation to interannual prediction? That is, the ENSO models and the ENSO statistics both show the same behavior! In that sense, it might be said that the simple coupled ocean-atmosphere ENSO-models are simulating or emulating the real system in a very adequate manner, or describing, at least, that part of the system described by the ENSO statistics. Thus, are the results indicating that the limit of predictability has been reached by the models.

(iv) Is the similarity of the ENSO modelling and observational results indicative of the modelling and observing of an incomplete system? From Fig. 2, it is clear that the ENSO models are not global. In fact, they do not take into account major parts of the global annual cycle such as the monsoon circulation or the transition to the asymmetric heating distributions prior to the monsoon. It was noted earlier that Normand (1953) showed that the monsoon anomalies precede variations in ENSO statistics in a much stronger manner than the reverse.

(v) Why is there a partial return of predictability following the spring demise? In both the model results shown in Fig. 4 and in the SOI correlations of Fig. 3, the correlation coefficient appears to rebound slightly after the major spring reductions. Whereas the increase is relatively minor it is interesting to contemplate how a system can increase its predictability.

These questions will be addressed in subsequent discussion.

4. The Annual Cycle of ENSO

Perhaps the most graphic description of the annual cycle of heat sources and sinks comes from the distribution of the outgoing longwave radiation (OLR) measured by satellite. Figure 5 shows the annual cycle of the OLR in terms of mean monthly distributions as a function of longitude and latitude. Solid black regions indicate infrared irradiances of less than 220 W m^{-2}. Hatched areas show irradiances greater than 300 W m^{-2}. In the Pacific-

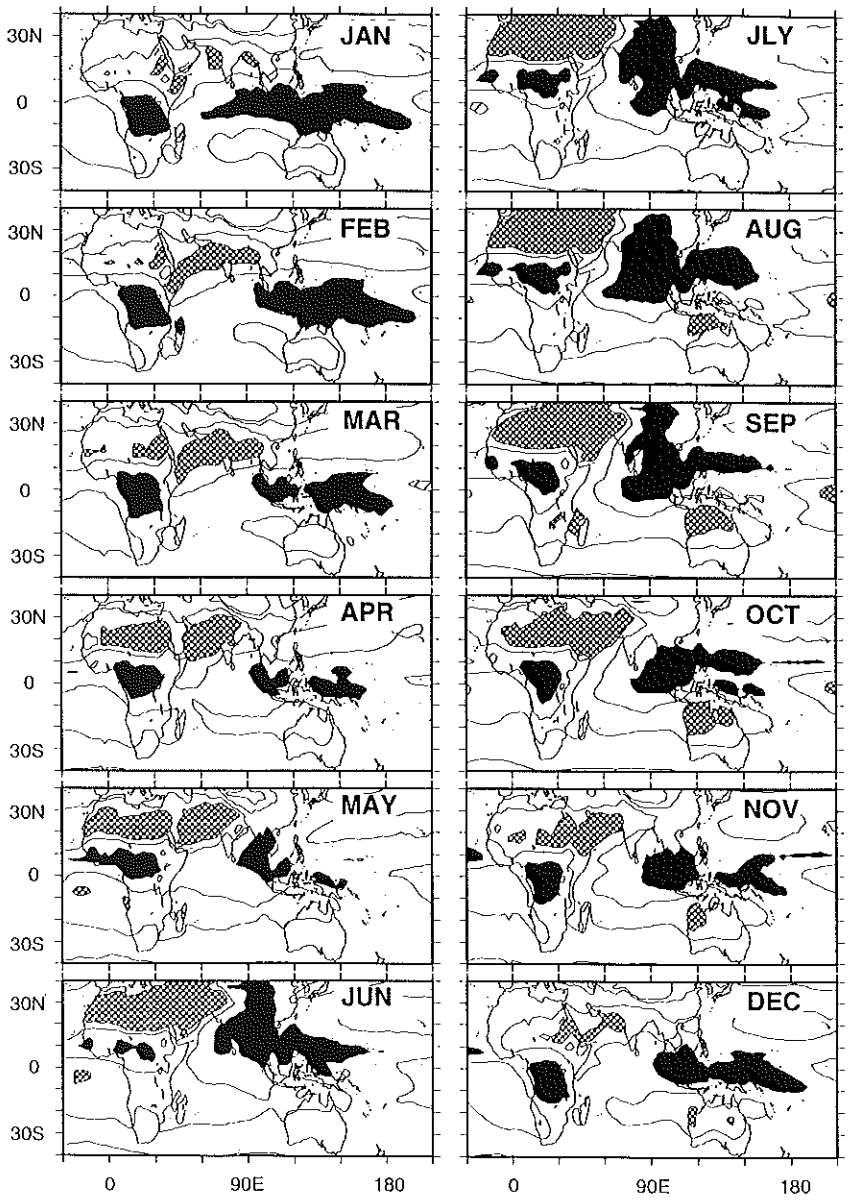

Fig. 5. The annual cycle of the outgoing longwave radiation (OLR) in terms of the long term monthly averages. In the Pacific-Indian Ocean region, the minima in OLR (correlated with maximum convection, and, thus, precipitation) exists in the eastern Indian Ocean and the western Pacific Ocean. Through spring and early summer, the locus of minimum OLR moves northward to East and South Asia. However, over North Africa and the Middle East, the maximum in OLR (indicating radiational cooling to space) exists as a very persistent feature throughout the year. In summer, the flux over the deserts increase in value by 30 W m^{-2} more than winter indicating an even greater loss of radiation to space

Indian Ocean region, the locus of OLR minima (and, thus convection) moves northward from the warm pool regions to East and South Asia between the boreal winter and summer and in the reverse direction during the other half of the year. However, over North Africa and the Middle East, the maximum in OLR (indicating regionally large radiational cooling to space) exists as a very persistent feature throughout the year. In fact, in summer, the extrema increase their values by 30 W m^{-2} to provide a much stronger radiative loss to space. This eastern hemisphere radiative heat sink is the most persistent climatological feature on the planet. Thus, as well as showing a strong annual cycle and migration of heating centers, the persistent regions of radiational cooling show that there is a complicated annual cycle of the gradients of latent and radiative heating (Webster, 1994). Between March and April, the magnitude of the OLR along the equator begins to increase suggesting a weakening of convection. On the other hand, while the along-equator heating gradient decreases, the monsoon heating is rapidly increasing as indicated by the growth of convection to the north of the equator between May and June. However, it appears that it is the decrease of heating along the equator that coincides with the timing of the predictability barrier rather than the increase in the monsoon circulation.

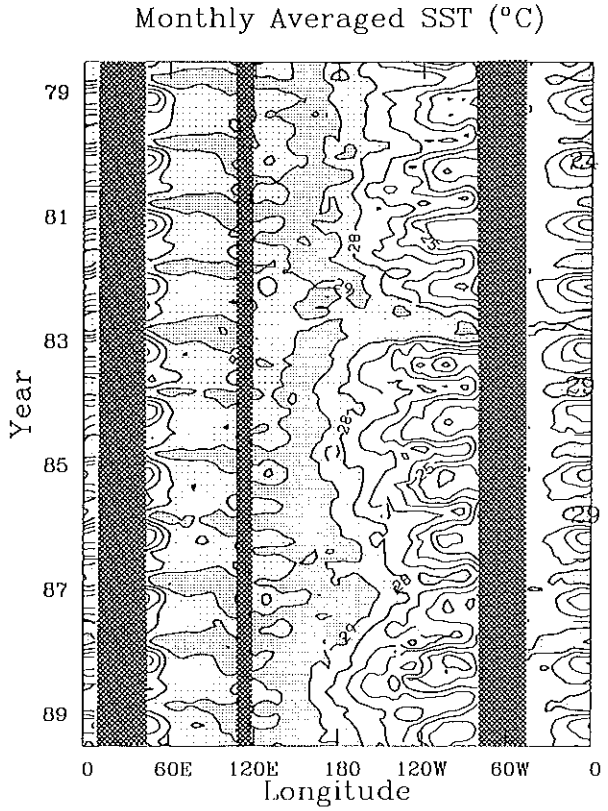

Fig. 6. The SST variation (°C) across the Pacific Ocean averaged between 5° N and 5° S for the period 1978 to 1989. Temperatures greater than 29 °C are heavily stippled. Lighter stippling refers to 28 °C water. The Indian Ocean shows very little interannual variability compared to the Pacific Ocean where warm events occur in 1982/1983 and 1987. However, the annual cycle is very apparent in the Pacific ocean as well as the Indian ocean. During the boreal spring there is a considerable relaxation of the SST gradient across the basin. The maximum longitudinal SST gradient occurs in summer. The warm events appear to be extensions of the annual cycle

Figure 6 shows a ten year time section of the SST around the equator. The shaded regions denote the land areas of Africa, Indonesia and South America, respectively, from east to west. Both the Atlantic and Indian oceans are dominated by a strong annual signature. In the Pacific ocean, superimposed on a fairly strong annual cycle, is a significant interannual variability with warm events (eastward extensions of the western Pacific warm pool) occurring in 1982/1983 and 1987. During the other years in the Pacific Ocean, especially in the east, there is an annual cycle that is similar in magnitude and phase to the Indian Ocean (see also Fig. 17). Longitudinal SST gradients relax from a maximum of about 6–7 °C across the Pacific basin in summar to about 3 °C in March–April. The 1982/1983 and 1987 warm events appear as extensions or amplifications of the seasonal relaxation of the pressure gradient.

Figure 7 shows a schematic of the flow associated with the low latitude and subtropical heating gradients for the June through August (JJA) period. The diagram is based on the seasonal means of the divergent parts of the wind field (Magaña, private communication). Estimates of the local values of the latent heating and radiative flux divergence are also shown (see Webster, 1994, for details).

Attempts have been made to model the annual cycle using coupled ocean-atmosphere models (e.g., Webster et al., 1994). The model used is a version of the Anderson-McCreary model (Anderson and McCreary, 1985). Its structure and

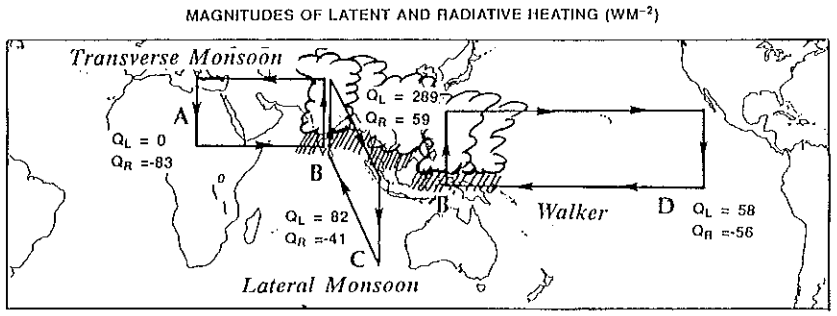

Fig. 7. Gradients in latent heat and radiative flux convergence between columns associated with the main branches of the summer monsoon and the near-equatorial circulation. Latent heating and radiative heating gradients between points A and B are 289 and 142 W m^{-2}; between B and C, 207 and 100 W m^{-2} and between B and D, 231 and 115 W m^{-2}. Note that the radiation gradients are about half the magnitude of the latent heating gradient and that the gradients of the two components are of the same sign. Thus, the total magnitudes between A and B, B and C and B and D are 431, 307 and 346 W m^{-2}. Hence, the heating gradients in the "transverse monsoon" (east-west) are somewhat greater than the gradients associated with the "lateral monsoon" (north-south). Clearly, the association of the North African desert regions with the monsoon cannot be ignored

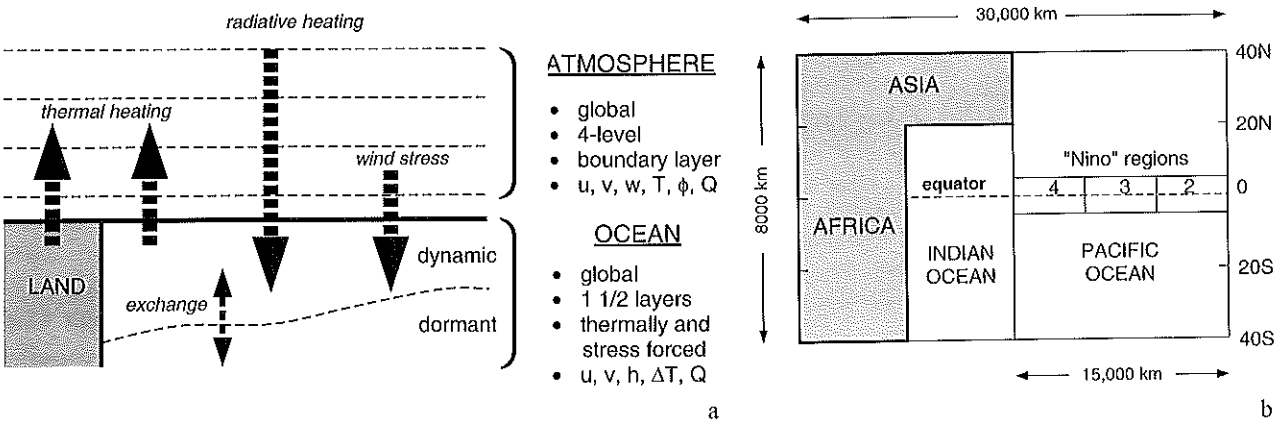

Fig. 8. (a) The structure of the coupled ocean-atmosphere model used in the numerical experiments. The atmosphere is a four-level, primitive equation, steady state model including a boundary layer. The ocean is a modified version of the Anderson-McCreary model. The models are coupled through and wind stress and through thermal heating from the land distribution. From Webster, et al. (1994). (b) The geometry of the coupled ocean-atmosphere model. The model consists of two oceans that resemble in size and geography the Indian and Pacific oceans. The Indian Ocean is surrounded by an Asian and an African continent. The Pacific and Indian Oceans are separated by an impermeable thin wall (solid meridional line). The three "Nino" regions are used to monitor the sea surface temperature variations in the Pacific Ocean. From Dixit, 1993 and Webster, et al. (1994)

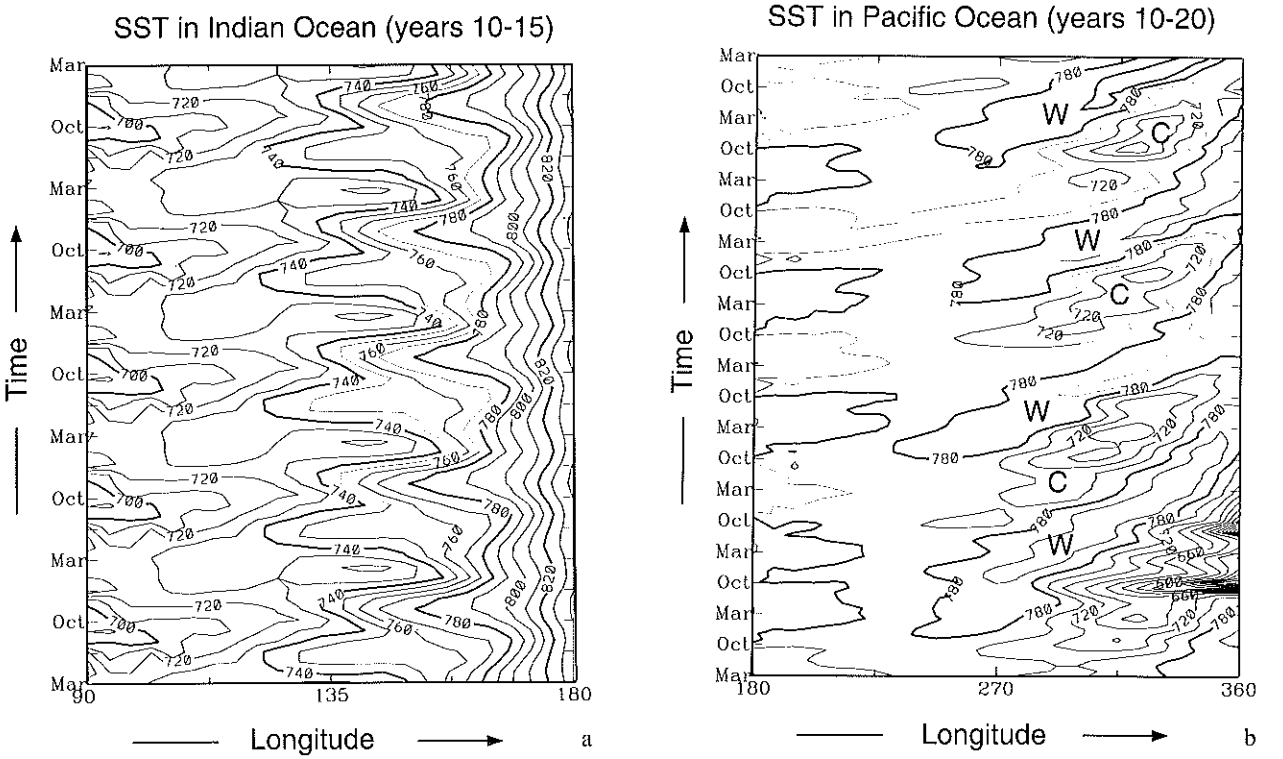

Fig. 9. (a) Time-longitude sections of the excess temperature of the model upper layer over the lower layer for the Indian Ocean. Isopleths are the model sea-surface temperature (SST: units hundreths of °C plus 20 °C). Time increases upward. The models are forced by the annual variation of solar radiation. Although the oceans are coupled by the interactive global atmosphere, the Indian Ocean is dominated by the regional annual cycle. (b) Same as Fig. 9a except for the Pacific Ocean. Even though an annual cycle is evident in the Pacific Ocean, there is substantial interannual variability that appears to be absent in the Indian Ocean

geometry are shown in Fig. 8a and b. The model is a coupled ocean-atmosphere two ocean basin model. The two oceans are surrounded by an "Africa-South Asia" continental structure. The model is driven by an annual cycle in radiative forcing, that, together with the model continental structure, imposes a strong asymmetric annual cycle to the forcing in both space and time. The solar heating heats the ocean and the land mass in an attempt to provide a similar heating distribution to the real climate system. A thin impermeable barrier (meridional solid line in Fig. 8b) separates the Pacific and Indian oceans.

Results of experiments with the coupled model are shown in Fig. 9a and b. The quantity plotted is the temperature excess of the ocean upper layer in hundreths of degrees Celcius above the 20 °C temperature of the lower ocean layer. Thus, an isotherm of 780, for example, indicates an upper layer temperature, or model SST, of 27.8 °C. There are a number of important results. First, the responses of the two ocean basins are completely different. On the one hand, the Indian Ocean is strongly phase locked to the annual cycle. The Pacific Ocean, though undergoes a variability which is primarily interannual, resembling, to some degree, the interannual El Niño cycle. Second, the annual cycle is somewhat weaker than observed in the Pacific Ocean (Fig. 6). This is a serious deficiency of many intermediate coupled model systems.

In summary, the annual cycle of the coupled system in the tropical region is very complicated. The principal reason is that the system is forced by waxing and waning symmetric and asymmetric heating functions about the equator. Furthermore, the symmetric and asymmetric components appear to be almost in quadrature with one another.

5. Hypotheses

Webster and Yang (1992) suggest two possible reasons why the observed correlation decrease of the SOI corresponds to the decrease in forecast skill of the coupled ocean-atmosphere models. Each hypothesis involves the annual cycle of the coupled system. The two hypotheses are not mutually exclusive.

5.1 The First Hypothesis: Robustness of the Near-Equatorial System

The first hypothesis rests on the similarity of the observed and modeled correlation curves shown in Figs. 3a and 4a, b, respectively. Specifically, the first hypothesis states:

The coupled prediction models are exhibiting an inherent predictability limit of the coupled ocean-atmosphere system. The inherent limitation on predictability is determined by the frailty of the near-equatorial circulation in the boreal spring during which time random errors grow at their most rapid rate of the year.

The frailty of the system is determined by the annual cycle of the near-equatorial pressure gradient (Fig. 3b). Frailty, in this sense, means that the overriding body forces on the system (i.e., the along-equator pressure-gradient force) is particularly weak compared to other times of the year. At this time, the equatorial regions may be easily influenced by small perturbations or error growth as the basic magnitude of the near-equatorial flow is closest to the magnitude of random perturbations. In other words, the signal-to-noise ratio is small.

Perturbations may arise from many sources. From a modelling perspective, errors may occur in the initial data. From a phenomenological perspective, the influence could come from non-equatorial sources not included in the ENSO statistics or in the ENSO type models and from small scale stochastic events. Whatever the influence (external or internal), the near-equatorial system is at its most vulnerable state, susceptible to perturbation and, thus, chaotic error growth during the boreal spring.

Figure 10 shows a schematic explanation of the robustness-frailty oscillation of the near-equatorial system. The top panel shows the ENSO cycle oscillating between two regimes. The restraints of ENSO are characterized by the wall on either side of a potential well. However, the height of the walls (the "robustness" of the system) is determined by the annual cycle. During the boreal spring, the annual cycle is such that the walls are low and the restraint is weak (see Fig. 3b). At this stage the climate may wander into other states. This state is referred to as "frail". During the boreal fall and winter, the annual cycle is strong

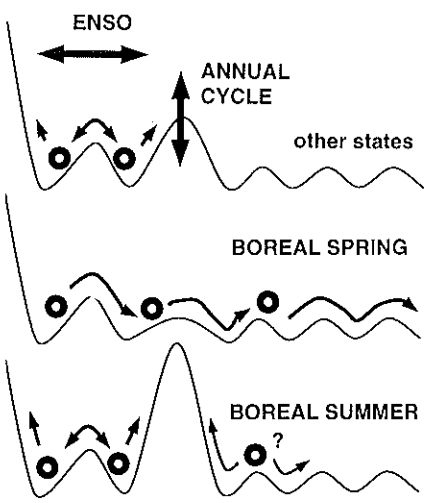

Fig. 10. Schematic representation of the first hypothesis or postulate of the boreal spring correlation decrease. The top panel shows the ENSO cycle oscillating between two regimes. The restraints of ENSO are characterized by the walls on either side of the potential well. However, the height of the walls (the "robustness" of the system) is determined by the annual cycle. During the boreal spring, the annual cycle is such that the restraint is weak (see Fig. 3b) and the climate may seek other states. We refer to this state as "frail". During the boreal summer, the annual cycle is strong or "robust". Whatever climate state, the system has wandered into during the boreal spring is retained until the system returns to frailty during the following spring. The influence of external forcing on the system is part of the second hypothesis

or "robust". The climate state the system has wandered into during the boreal spring is retained within the more robust system until the system returns to frailty during the following spring.

To test the influence of the annual cycle on the robustness of the Pacific Ocean basin system requires very careful modelling. In fact, if the latter speculation is correct, the models will have to have substantial vertical structure. In Section 6, the results of experiments designed to test whether there is an annual cycle of random error growth will be shown. Monte Carlo techniques are employed. If the robustness of the system is a function of the annual cycle, then the forecasts will show a larger ensemble spread only at certain times of the year.

5.2 *The Second Hypothesis: Influence of External Factors*

The second hypothesis states that:

The loss of predictability within a coupled ocean-atmosphere model, or in near-equatorial statistics, arises from the systematic influence of phenomena not included in models or in the diagnostics of the ENSO coupled ocean-atmosphere system.

If such phenomena can be identified, and if such systems possess an inherent predictability of their own, their identification may be important in allowing the boreal spring predictability barrier to be bridged.

Webster and Yang (1992) sought external influences that would peak at the time of the predictability barrier. There are a number of candidates:

(i) The evolving annual cycle of large-scale heat sources and sinks in the tropical and subtropical belt are shown in Fig. 5. Figure 5 does not show the convection around central America which also shows a distinct annual cycle. The filter used here on determining the importance of external heat sources and sinks is that they possess a demonstrated lead of the SOI. This association is not clear for heating over central America. Furthermore (see Fig. 17), the variability of the central American asymmetric heating is in phase with the Walker circulation and not in quasi-quadrature like the monsoon heating.

(ii) The evolving summer monsoon over South Asia. During late spring the boreal summer monsoon is in its strongest growing phase. Although this maximum growth occurs later than the occurrence of the predictability barrier, the near-equatorial system appears weakest and most susceptible to influence at that time. Furthermore, there exists very strong variability in the monsoon from one year to the next; and

(iii) The influence of anomalous high latitude circulation patterns on the tropics. For example, the extent of the previous winter's sea-ice in the northern oceans and snow cover over Eurasia may produce large-scale circulation differences and weather patterns that could influence the near equatorial circulation during the boreal spring.

Returning to Figs. 3 and 4, it appears that the predictability demise commences in March and continues through May. During this period, the heat sources and sinks over the western Pacific Ocean and the eastern Indian ocean are undergoing their strongest and most rapid change

(Fig. 5). Heating tends to develop a strong asymmetric component as the locus of maximum heating moves northwards towards South Asia. However, Webster and Yang (1992) showed that the monsoon does not begin its most rapid growth until late April or early May. Thus, in terms of timing, candidate (i), the evolving state of the near-equatorial coupled system, is probably more associated with the predictability barrier than candidate (ii), the growth of the monsoon. Furthermore, it should be noted that the development of the asymmetric heating fields are not contained in the ENSO-type models.

Webster and Yang (1992) showed that there is considerable variability in the phase and amplitude of each monsoon year. For example, the average seasonal kinetic energy over south-east Asia in 1986 summer is about 30% greater than 1987. Thus, the summer monsoon, with a strong interannual variability, is in its rapid growth phase after the correlation decrease has commenced and when the near-equatorial system is weakest. The maximum of the winter monsoon, on the other hand, occurs at the time of the maximum amplitude of the pressure gradient, and, thus, the maximum strength of the near equatorial circulation.

Webster and Yang (1992) configured a monsoon index to differentiate between anomalously strong and weak boreal summer monsoons. Because precipitation is a difficult parameter to obtain and may be extremely biased geographically an index based on vertical wind shear over the South Asian region was developed. The choice of vertical shear as a surrogate for monsoon strength has a sound theoretical basis. Webster (1972) and Gill (1980) have shown that the magnitude of the first baroclinic mode is proportional to the magnitude of the heating. By extension, the vertical shear should provide a large scale index of precipitation. With this index, strong and weak monsoons were separated. For example, 1984, 1985 and 1986 were strong monsoon years. 1979, 1982, 1983 and 1987 were weak monsoon years.

Figure 11a and b (from Webster and Yang, 1992) shows the composite OLR and 850 mb and 250 mb anomalous zonal wind distributions for the strong and weak monsoon summers respectively. Coherent and large scale signatures match both categories of monsoon intensity in all three quantities. Concentrating on the 850 mb level, enhanced trade winds over the Pacific Ocean are associated with the strong monsoons while weakened trades are associated with weak monsoons. Thus, coherent simultaneous linkages appear to exist between the anomalous monsoons and the Pacific Ocean, and thus the region explicitly modeled by coupled ocean-atmosphere ENSO models (Fig. 2). Clearly, if the monsoon regions were not included in the geography of the model, then important variations in the wind forcing of the Pacific Ocean basin would be missing. Thus, as wind stress is a major communicating factor between the atmosphere and the ocean, a major influence on the El Niño cycle may be absent if the influence of the monsoon were ignored.[1]

Although Fig. 11 shows strong relationships between the monsoon and the low level wind field in the Pacific Ocean (and thus possibly with ENSO), it adds little to the solution of the predictability problem. Such a solution would require precursors for the strong and weak monsoon periods to exist across the boreal spring predictability barrier. From Fig. 3, it is clear that the SOI is not the most useful index for the task. However, given the contemporaneous relationship between anomalous monsoon and Pacific basin winds, in addition to the lagged relationship of the SO to the monsoon (Walker, 1923, 1924; Normand, 1952), it seems reasonable to seek precursors of the anomalous boreal summer monsoon.

Figure 12 shows the annual cycle of the mean monthly 850 and 200 mb zonal flow over the South Asian region. Prior to strong monsoons, the upper tropospheric anomalous zonal flow is weak; some 5–10 $m\,s^{-1}$ more easterly than prior to a weak monsoon. However, at 850 mb the signal is indistinguishable prior to the spring and summer. That is, precursors exist in the upper troposphere as long ago as the previous boreal winter although only later near the Pacific Ocean ocean-atmosphere interface. However, the signal does not appear to influence the trade wind regime of the Pacific Ocean until roughly the time of the occurrence of the predictability barrier.

The upper tropospheric precursors appear to be part of very large scale anomalous circulation

[1] Chengfeng Li and Professor M. Yanai have extended the analysis of Webster and Yang (1992) through 1992. They find very similar associations between circulation characteristics, SST and OLR and the monsoon strength.

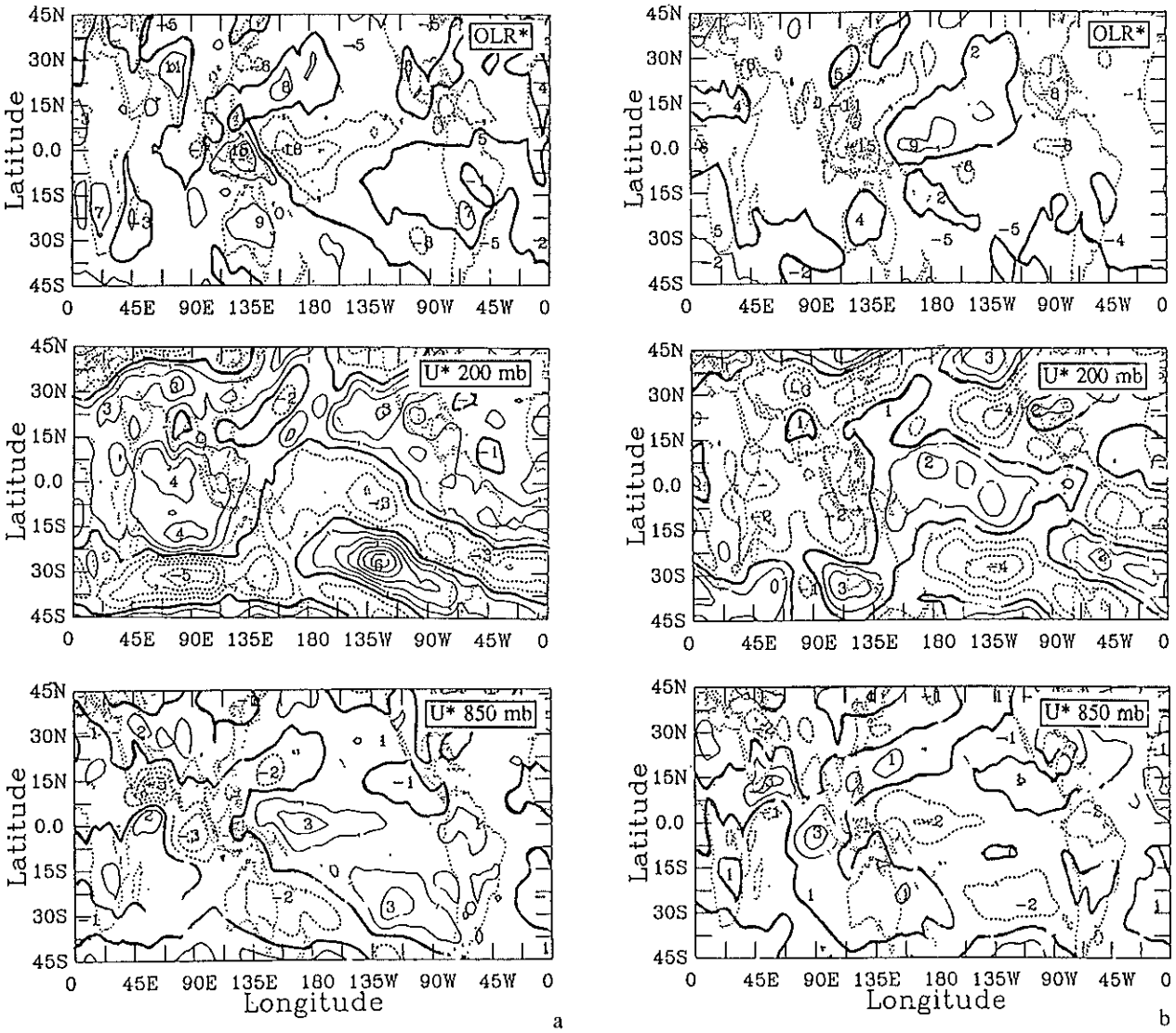

Fig. 11. (a) Composites of the anomalous OLR-field (upper panel), and the anomalous 200 mb and 850 mb zonal wind fields (middle and lower panel) for the "weak" monsoon years (1979, 1982, 1983, 1987) defined using a monsoon circulation index (Webster and Yang, 1992). Contours are 5 W m^{-2} for OLR and 1 m s^{-1} for the wind fields. The zero contours are bold. (b) Composites of the anomalous OLR-field (upper panel), and the anomalous 200 mb and 850 mb zonal wind fields (middle and lower panels) for the "strong" monsoon years (1984, 1985, 1986) defined using a monsoon circulation index (Webster and Yang, 1992). Contour intervals are 5 W m^{-2} for OLR and 1 m s^{-1} for the wind fields. The zero contours are bold

patterns. Webster and Yang (1992) showed that the December-February and March-May periods possessed anomalous patterns of winds with considerable coherence and which were associated with strong and weak monsoons (Fig. 13). Such patterns showed that the eastern hemisphere to the north of the equator were dominated by anomalous easterlies before a strong monsoon and anomalous westerlies before a weak monsoon. It should be noted that these upper tropospheric precursors of the anomalous monsoons exist before and across the boreal spring predictability barrier defined earlier.

It is interesting to note that the patterns shown in Fig. 13a and b are very similar to the patterns found in the numerical experiments of Vernekar et al. (1994) for anomalous snowfall over Eurasia during the previous winter. These patterns were produced by numerical experiments where observed extremes of snowfall were used as initial conditions in general circulation model simulations.

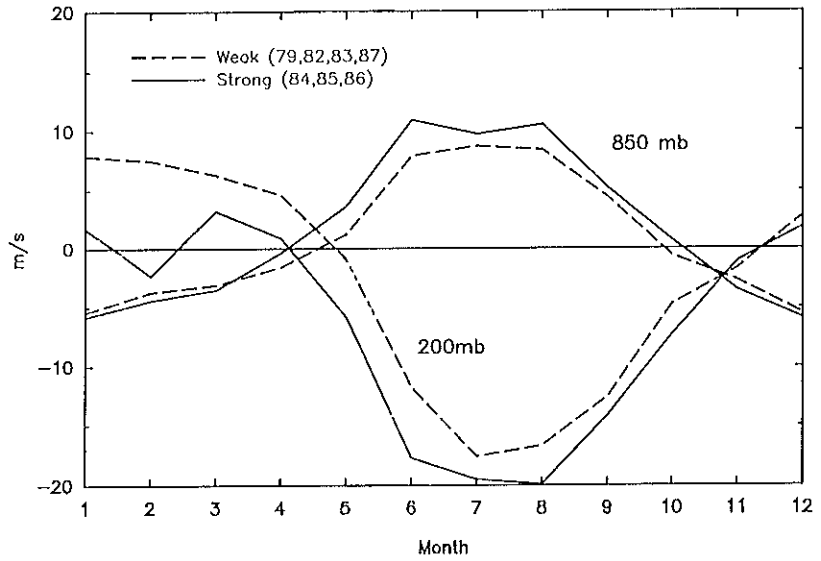

Fig. 12. Composite annual variation of the 850 mb and 200 mb zonal wind component wind in the South Asian region (5° N–20° N, 40° E–110° E) for years defined by "strong" monsoon (solid curves) and "weak" monsoons (dashed curves). Differences are apparent as early as the previous winter. It would appear that "strong" broad-scale monsoon years are preceded by very weak winter upper-tropospheric winds. Note that the signal is not apparent in the lower troposphere at times earlier than the summer

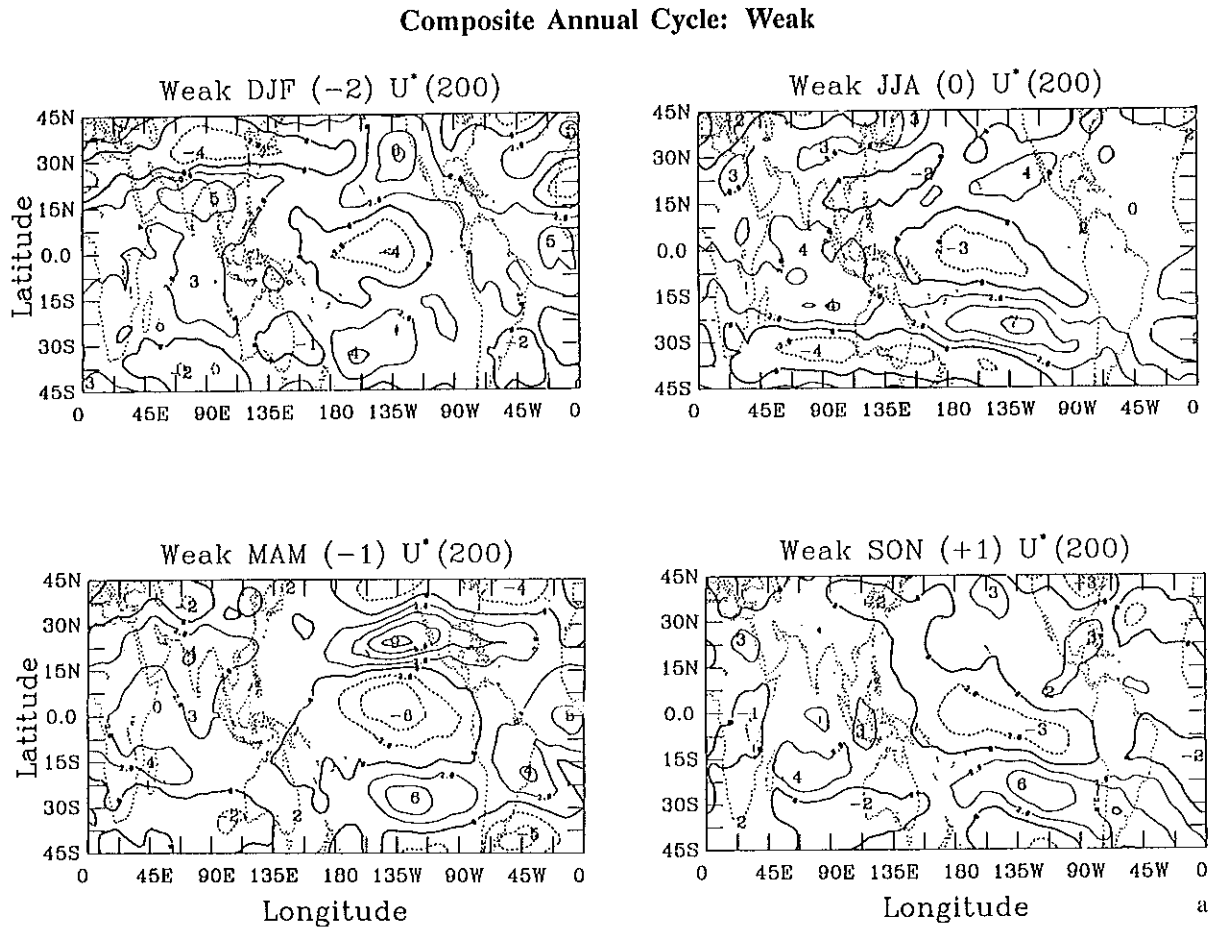

Fig. 13. (*Continued*)

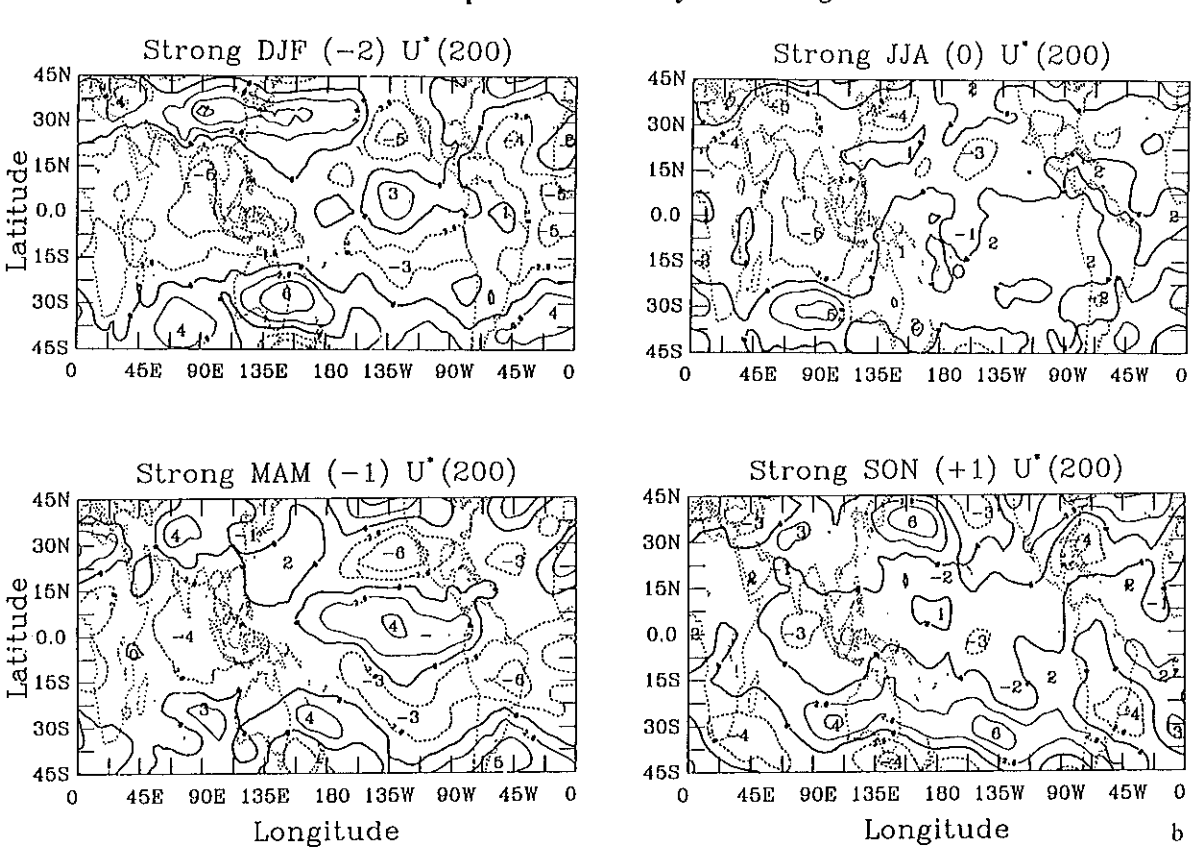

Fig. 13. (a) Composite annual cycles of the 200 mb zonal wind component for the years defined by a weak summer monsoon. Composite mean seasonal fields are shown from the previous winter (DJF: −2 seasons) to the following winter (DJF: +2 seasons). Contours interval are 1 m s^{-1} and negative values are dashed. Webster and Yang (1992). (b) Same as Fig. 13a except for the years defined by a strong monsoon. Webster and Yang (1992)

In summary, the second hypothesis deals directly with the influence of the monsoon on the Pacific basin lower tropospheric wind field. The hypothesis is described schematically in Fig. 14.

6. Modeling Error Growth in an ENSO System: Testing the First Hypothesis

To test the first hypothesis, it is necessary to show that there is an annual cycle in error growth in the coupled ocean-atmosphere system. Clearly, this is a difficult test to perform using data, so models must be used to perform the task. Even with models the procedure is rather difficult and requires a carefully designed set of experiments. As the systems considered here are nonlinear, it is necessary to perform a large number of experiments to ensure that a statistically reasonable conclusion can be reached.

The modified Anderson-McCreary model (Webster et al., 1994; Dixit, 1993; Dixit and Webster, 1992: Fig. 8) is used. The basis of the experiment is a fourteen year control of the coupled ocean-atmosphere system. During the eleventh year of the control run, twelve random perturbations to the initial conditions (provided by the control run) were made at the beginning of each calendar month to produce a total of 144 experiments over the next model year. The spread of the ensemble for each month provides an assessment of the annual cycle of error growth in the system.

There are two caveats that should be taken into account when these results are considered. The first is that in this series of experiments the model is not run in fully independent mode. A complete model would allow for full feedbacks between all of its components. The version of the model used

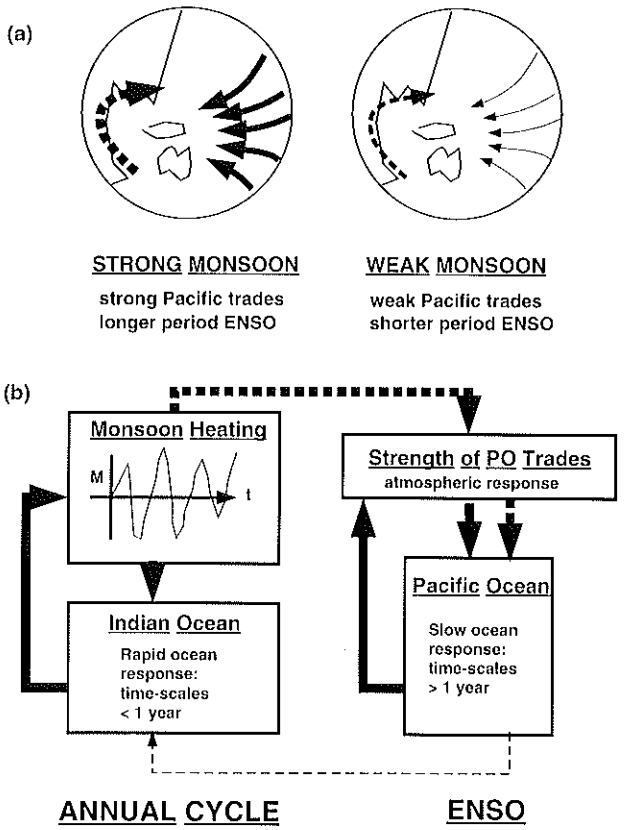

Fig. 14. Schematic of the second hypothesis: (a) The influence of monsoon variability on the Pacific basin. When the monsoon is strong, the trades in the Pacific Ocean are stronger. Conversely, when the monsoon is weak, the trades are weak. It is anticipated that the stronger trades will increase the period of ENSO by retaining the head of warm water in the western Pacific. Weaker trades, on the other hand, will allow the head to relax and invoke a more rapid onset of a warm event. (b) A flow diagram of the interaction of the monsoon and interannual variability. The annual cycle and ENSO are considered as two separate systems. The monsoon and the Indian ocean are tied into a strong annual cycle. The Pacific Ocean undergoes a slow ENSO oscillation. However, on an annual basis, the monsoon influences the strength of the trades and, thus, imparts an annual variability on the Pacific Ocean. However, from year to year, the amplitude of the monsoon is variable and the modified trades impart variability onto the ENSO cycle

here, on the other hand, is run in a constrained format where certain feedbacks are not allowed. Whereas the global ocean and atmosphere are allowed to interact freely, the land forcing is a prescribed function of the solar heating and the zonally averaged wind field is provided by a nonlinear zonally symmetric model of Webster and Chou (1982). Like many coupled ocean-atmosphere models of the intermediate type, the model produces an oceanic annual cycle that is somewhat weaker than that observed. Probably, the lower amplitude is a result of the atmospheric model producing weak trade winds: an inherent problem of linear steady state atmospheric models (Dixit, 1993).

Figure 15 shows a subset of the results from the Monte Carlo experiments for the SST in the Niño 2 region, the location of which is shown in Fig. 8b. The curves represent differences between the predicted SST and the control experiment. The control SST is shown as the broad gray curve in the figure. For clarity, only half of the 144 runs are displayed with sets of experiments commencing every two months following January of the eleventh year. The most obvious feature of the results is that the anomalies maximize at the same time of the year irrespective of when a particular experiment commences. For example, for the January set, major deviations do not occur until the March-May period of the twelfth year. This is the same period that all other predictions also deviate. Furthermore, the variability of the sets of realizations increases with time. Maximum variation appears to occur at the time of the most rapid change of SST especially when the SST heads into a minimum phase of SST in the eastern Pacific Ocean and at the extrema of the semiannual variability of SST (minor peaks of the SST curve). Most probably, the temperature deviations of the realizations occur because of induced changes in the phase of the El Niño cycle and of the annual cycle by the random perturbations.

In summary, the Monte Carlo experiments indicate that there are preferred periods of the annual cycle where errors grow more rapidly than others especially when then SST is undergoing significant changes during the annual cycle. However, it is difficult to relate readily the variability noted here with that considered from diagnostic studies or from ENSO-type models because of the two weaknesses of the model noted above. Further advances and considerations must await attention to these two problems.

7. Modeling the Influence of the Monsoon on ENSO: Testing the Second Hypothesis

It may be inferred from the previous section that there is little hope of extending coupled system predictability on interannual time scales with

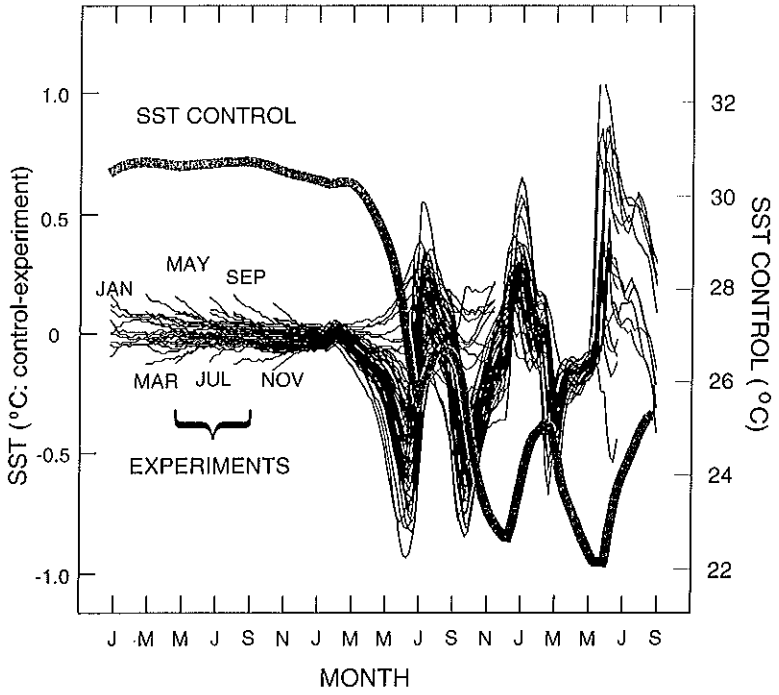

Fig. 15. Preliminary results of the Monte Carlo experiments with the coupled model. Twelve randomized experiments were commenced at the beginning of each month during the eleventh year of integration totalling 144 experiments. For clarity only half of the 144 experiments are shown. The anomalous SST in the Niño 3 region (see Fig. 8b) are plotted (left ordinate). The control SST in the same region is shown as the board gray curve (right ordinate). Irrespective of when the experiments were commenced, the greatest deviations of all of the ensembles occur at the same time of the year

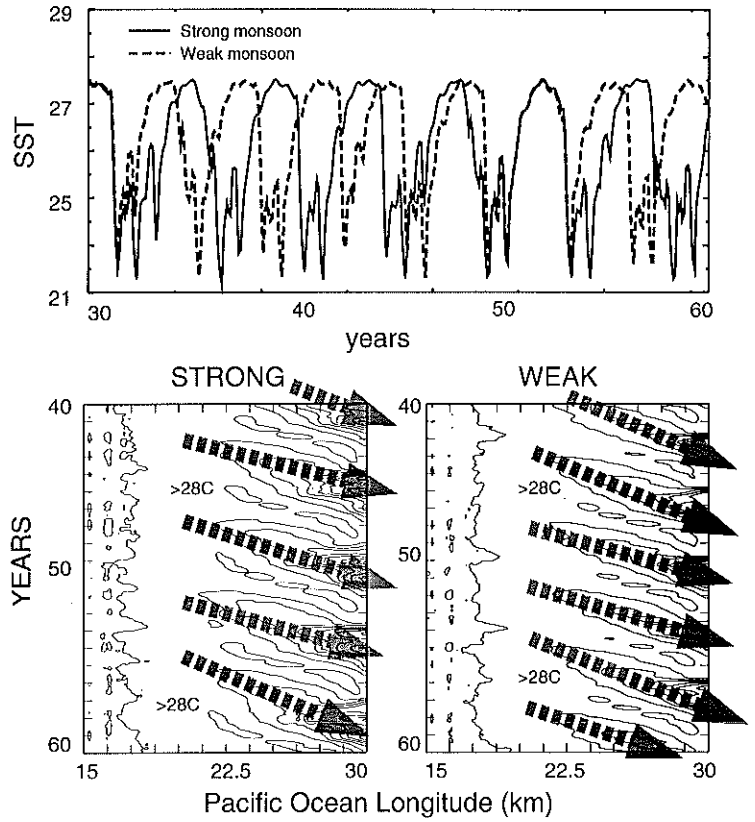

Fig. 16. Results of the coupled ocean-atmosphere model described in Fig. 8. Upper panel shows the variation of SST in the Niño 3 region shown in Fig. 8b. Lower left panel shows a time-longitude plot of the SST in the Pacific Ocean over a 20-year period. Right-hand panel shows same plot for weak monsoon forcing. Arrows show propagation of warm events and indicate a longer period for strong monsoon forcing than for weak monsoon forcing

models that are limited to the modeling of the ENSO system alone. The restrictions on the predictive capability of the ENSO cycle probably result from the temporal correspondence of two circulation factors at the same time of the year; the "frailty" of the near-equatorial coupled system that is maximized at the time of most rapid growth of the monsoonal external forcing. If an

extension of interannual prediction is possible beyond the limitation imposed by the ENSO predictability barrier, it will have to take advantage of the extended monsoon signal, discussed above.

To test the second hypothesis that the variable amplitude of the monsoon modifies the phase of ENSO events, the two-ocean coupled ocean-atmosphere model described in Fig. 8 is used. In a series of experiments, the heating the "Asian" continent during summer is perturbed to produce strong or weak monsoons. The magnitudes of the heating anomalies are determined from time series of OLR over the South Asian region (specifically, along 80° E between 10° N and 20° N) from 1974 through 1989. Amplitude variations fall roughly in the range of $\pm 10\%$. Cases are shown for strong monsoon forcing and weak monsoon forcing. The upper panel in Fig. 16 compares the Niño 3 SSTs for a 30 year period. 20-year time-longitude sections along the equator are shown in the bottom panels. The period of ENSO changes significantly depending on the strength of the summer monsoon. Strong monsoon forcing appears to lengthen the period of ENSO while weak monsoons tend to shorten the period.

In summary, the results of the simple experiments confirm the observational results that the monsoon exerts considerable influence on the interannual variability of the Pacific basin and, thus, on the ENSO phenomena. Whereas a quantification of the feedbacks between the monsoon and ENSO has been achieved, the results were hinted at many years ago in the pioneering observational work of Walker (1923, 1924) and by Normand (1953).

8. Conclusions

8.1 Summary

This paper has considered physical processes that may be responsible for the intriguing decrease in predictability that occurs in the boreal spring in both model forecasts of ENSO and lagged correlations using low latitude indices computed from data. It was noted that the correlation decrease potentially limited forecasting usefulness to limits of from a few months to less than a year. As the correlation decrease is phase locked with the annual cycle, it would appear that the annual cycle plays a distinct role in settling the limits of interannual predictability.

Two hypotheses were posed to explain the seasonal correlation decrease. The first hypothesis was based on the observations that the decrease occurred at the time that the equatorial pressure gradient in the Pacific Ocean (in concert with the SST gradient) was at a minimum. At such times, the signal-to-noise ratio would be smallest and it was hypothesized that random error growth would occur rapidly relative to the deterministic signal. Initial experiments with a coupled ocean-atmosphere model using Monte Carlo techniques showed that there are preferred periods of error growth in the coupled system. The second hypothesis suggested that external influences (such as the rapidly growing Asian monsoon) could influence the near equatorial coupled system at the time when it was least resilient, such as following the boreal spring. Given the interannual variability of the intensity of the monsoon system, the late spring forcing of the Pacific Basin could impart strong variability on the basin-wide stress fields. Experiments with a coupled ocean-atmosphere model indicate that the asymmetric forcing associated with the monsoon varies the amplitude of the model's interannual variability. In fact, variations of $\pm 10\%$ in the amplitude of the monsoon altered the ENSO period by about $\pm 20\%$.

8.2 A Unified Hypothesis

It is clear that the two hypothesis are not mutually exclusive. In fact, it is possible to combine them. The key lies in the observation that the strength of the Walker Circulation and the monsoon circulation are nearly in quadrature. That is, while the Walker Circulation is approaching its weakest state, the monsoon is approaching its strongest, and vice versa. The combined hypothesis may be described in the following manner:

During the spring and early summer, the annual cycle of the near-equatorial pressure gradient becomes sufficiently weak that the Walker circulation becomes frail and random errors grow rapidly. At this stage, predictability of the system is reduced or lost. In the early summer, the rapidly growing monsoon system eserts a basin wide wind stress anomaly pattern to the frail Pacific Ocean near-equatorial system. The character of the stress field is determined by the magnitude and phase of the anomalous monsoon. Later in the year, as the Walker Circulation regains its intensity, but

possesses the special character provided by the modified coupled system, it imparts its character on the winter monsoon. In the following spring, the signal of the previous summer monsoon is lost in the near-equatorial system as the Walker Circulation weakens again. The time-scale of interannual variability in the coupled system is a combination of the basic time period of ENSO plus a rectification of the interaction of the monsoon and the Walker Circulation.

Figure 17 provides a schematic representation of the interaction of the monsoon and the Walker Circulation. To produce the figure, the OLR was separated into asymmetric and symmetric components about the equator (Webster and Yang, 1992). The upper panel shows the asymmetric component along 14° N plotted as a function of latitude. The shaded areas indicate OLR anomalies of -20, -30 and $-40\,W\,m^{-2}$. The lower diagram shows the symmetric component along the equator. Shades areas denote OLR values of 220 and 200 $W\,m^{-2}$. In the bottom panel the rapidly weakening Walker Circulation is evident. From Fig. 3b, this corresponds to the time of the predictability barrier. About a month later the monsoon increases its intensity very rapidly (upper panel). It is hypothesized that at this time the monsoon exerts its influence on the frail tropical regime. Later in the fall, as the summer monsoon weakens, the Walker Circulation increases in intensity and modifies the structure of the winter monsoon.

There may be an alternative explanation of the error growth during the boreal spring that is also consistent with the slight increase of predictability following the demise. During most of the year, the tropical ocean and atmosphere are strongly coupled and the climate trajectories that they find themselves in are joint trajectories. However, in springtime, as the winds across the Pacific Ocean decrease, it is possible that the ocean and the atmosphere become detached. Consider the state of the joint system prior to the boreal spring. Perturbations on the thermocline (signals of the propagating wave packets across the basin) are reflected in the surface topography and SST distribution and, hence, in the anomalous atmospheric circulation. Suppose that the basin wide winds decrease as they are observed to do at the same time each spring when the warm pool

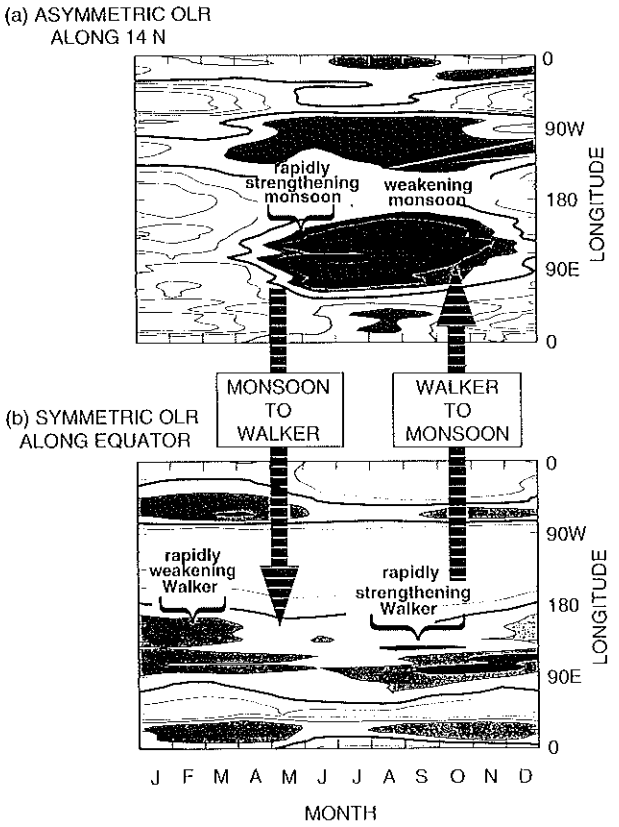

Fig. 17. Schematic diagram of the unified hypothesis. Upper panel shows asymmetric component of the OLR along 14° N; lower panel, symmetric component along equator. Shaded areas (convective maxima) show the asymmetric component (monsoon) and the symmetric component (Walker) to be nearly in quadrature. Between the boreal winter and spring, the Walker circulation weakens considerably. The ocean and atmosphere in the Pacific basin become "detached" with each following its own climate trajectory. External influences, in the form of the rapidly strengthening monsoon, perturb the Pacific basin by the application of anomalous stress. The recoupled system is now on a different or adjusted, although joint, climate trajectory

extends eastward (see Fig. 6). If the extension of the warm pool is due to the warming of the surface layer resulting from a reduction in evaporation and mixing, a weak, although stable, near-surface thermocline could develop across the entire Pacific Ocean. Thus, because of the development of the near-surface barrier layer, the variability of the SST may become independent of the variability of the thermocline and the ocean and the atmosphere could become effectively detached. At that stage, the atmosphere and the ocean, now separated by the barrier layer, would be free to move off the joint trajectory and into their own.

The speculation has the advantage of offering an explanation of why there is a small return of predictability in the observed lagged correlations (Fig. 3) and the models (Fig. 4) after the initial spring decrease. As the winds increase in summer and the shallow near-surface thermocline is eroded, the signal on the thermocline (albeit relaxed and evolved during the interim period) reasserts a correlation with the SST and the atmosphere. The atmosphere it finds, however, is now uncorrelated and may be modified substantially by other events such as anomalously strong or weak monsoons, etc.. Thus, the reasserted system correlation is weak. The speculation is also testable with both models and observations. The TOGA-TAO buoy data can provide long-term station data from which the annual cycle of the vertical structure can be obtained. Some buoys have been maintained in the same location since the early 1980's.

Finally, it should be mentioned that there appears to be some evidence that there are precursors to the strength of the monsoon and that they span the predictability barrier. Thus, assuming that the influence a strong or weak monsoon will have on the near-equatorial coupled system is understood, it may be possible to extend the range of prediction across the boreal springtime barrier. A speculated sequence of events taking into account both the speculation regarding the detachement of the ocean and the atmosphere and the role of external forcing is shown in Fig. 18.

8.3 Future Work

There are three main directions for future work. In the first place, the observational evidence for precursors of anomalous monsoon circulations must be substantiated. A second direction is to understand the physical relationships that appear in the data and the models. Furthermore, models must be developed that reflect the physical mechanisms of the annual cycle and interannual variability.

Even though the relationship of upper tropospheric winds in the eastern hemisphere with the subsequent monsoon appear strong, they only come from a thirteen year data set. The reason for this limitation is that thirteen years is the maximum length of a more or less unified data set generated by operational centers. Before that period, models were initialized in ways that rendered the resulting data fields effectively useless for research into low latitude phenomena.There is some hope that these data sets will be subject to reanalysis using a common system, although even reanalysis will only incrementally increase the length of the sets. Probably, it will be necessary to return to the original data sets and perform conventional analyses. Such a project may be fruitful as high quality and long-term wind data sets exist over South Asia and the Indian subcontinent.

If a precursor for strong and weak monsoons remains a pervasive signal following a more

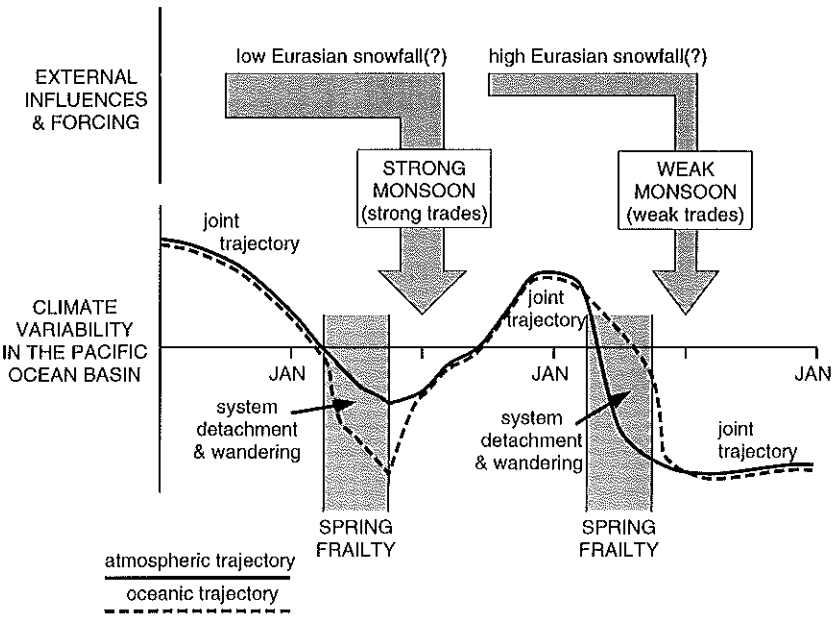

Fig. 18. Detail of the unified hypothesis showing the combined effect of internal frailty and external influence on the climate of the Pacific Ocean basin. During the weak circulation period of spring, the ocean and atmospheric components become detached. This structure is distinctly different to the highly coupled state that existed before the spring. Anomalous monsoons, which apply differential wind stress to the Pacific basin, coupled the ocean and the atmosphere together again. However, the joint trajectory is now different as the system component wandering has introduced errors into the system. It is hypothesized that some predictability in the system will be retained through spring if there is a resilient oceanic signature on the thermocline

exhaustive observational analysis, it would be necessary to consider why there is an anomalous large-scale wind field existing in the eastern hemisphere in the winter and spring prior to the summer monsoon. Is the anomaly produced by simple relationships caused by anomalous boundary conditions either over the continental regions or the oceans such as suggested by Verneker et al., (1994)? An extreme range of Eurasian snowfall was used in finding a discernible signal in the subsequent monsoon strength. It would be valuable if the experiments were repeated with the observed variability of year-to-year snowfall.

Finally, the state of coupled ocean-atmosphere models requires considerable attention. If the suggestions made in this paper are correct and the annual cycle of the coupled ocean-atmosphere system is important in interannual variability, then a minimal requirement for coupled models is that they emulate the annual cycle properly. Unfortunately, this is not the case. A *cause celebre* for the modeling community is the improvement of coupled models to produce more adequate representations of the annual cycle.

Acknowledgments

Funding for this research was obtained through grants from the DOC/NOAA Office of Global Programs (DOC NA26GPO 12201) and the Climate Dynamics/Atmospheric Sciences Division of the National Science Foundation (ATM-9214840). I have benefited from discussions with T. N. Palmer of the European Centre for Medium Range Weather Forecasting regarding the Monte Carlo experiments and with R. Lukas of the Department of Oceanography, University of Hawaii for general discussions of the role of monsoons in ocean-atmosphere interaction. I am indebted to N. N. Nicholls of the Bureau of Meteorology Research Centre for pointing out the phase differences between the predictability barrier and the growth of the monsoon. His comments on an earlier version of the paper led to the combined hypothesis. Finally, I appreciate the discussions and help from my colleagues H.-R. Chang, V. Magaña and J. Goldstein of PAOS.

References

Anderson, D., McCreary, J., 1985: Slowly moving disturbances in a coupled ocean-atmosphere model. *J. Atmos. Sci.*, **42**, 615–629.

Battisti, D. S., Hirst, A. C., 1989: Interannual variability in a tropical atmosphere-ocean model: Influence of the basic state, ocean geometry and nonlinearity. *J. Atmos. Sci.*, **46**, 1687–1712.

Bjerknes, J., 1969: Atmospheric teleconnections from the equatorial Pacific. *Mon. Wea. Rev.*, **97**, 163–172.

Cane, M. A., 1991: Forecasting El Niño with a geophysical model, Chapter 11. In: Glantz, M., Katz, R., Nicholls, N., (eds.) *Teleconnections Connecting World-Wide Climate Anomalies*, Cambridge: Cambridge University Press, 345–369.

Cane, M. A., Zebiak, S. E., 1985: A theory of El Niño and the southern oscillation. *Science*, **228**, 1085–1087.

Dixit, S., 1993: The role of the mean atmospheric flow in interannual predictability, PhD Thesis, The Department of Meteorology, The Pennsylvania State University, 245 pp.

Dixit, S., Webster, P. J., 1992: The role of the mean flow in low-frequency variations in the Pacific Ocean. Proceedings of the Climate Diagnostics Workshop, October, Norman, Oklahoma.

Gill, A. E., 1980: Some simple solutions for heat induced tropical circulations. *Quart. J. Roy. Meteor. Soc.*, **106**, 447–462.

Hao, Z., Neelin, J. D., Jin, F.-F., 1993: Nonlinear tropical air-sea interaction in the fast-wave limit. *J. Climatol.*, **6**, 1523–1544.

Latif, M., Graham, N. E., 1991: How much predictive skill is contained in the thermal structure of an OGCM? *TOGA Notes*, **2**, 6–8.

Neelin, J. D., 1991: The slow sea surface temperature mode and the fast-wave limit: Analytic theory for tropical interannual oscillations and experiments in a hybrid coupled model. *J. Atmos. Sci.*, **48**, 584–6065.

Neelin, J. D., Jin, F.-F., 1993: Modes of interannual tropical ocean-atmosphere interaction. – A unified view: Part II. Analytic results in the weak coupling limit. *J. Atmos. Sci.*, **50**, (in press).

Nicholls, N. N., 1984: The southern oscillation and Indonesian sea surface temperature. *Mon Wea. Rev.*, **112**, 424–432.

Normand, C., 1953: Monsoon seasonal forecasting. *Quart. J. Roy. Meteor. Soc.*, **79**, 463–473.

Philander, S. G., 1990: *El Niño and the Southern Oscillation.* San Diego: Academic Press, 289 pp. (International Geophysics Series, **46**).

Rasmusson, E. M., Carpenter, Y. H., 1983: The relationship between the eastern Pacific sea surface temperature and rainfall over India and Sri Lanka. *Mon. Wea. Rev.*, **111**, 354–384.

Rasmusson, E. M., Wang, X., Ropelewski, C. F., 1990: The biennial component of ENSO variability. *J. Marine Systems*, **1**, 71–96.

Shukla, J., 1987a: Interannual variability of monsoon. In: Fein, J. S., Stephens, P. L. (eds.) *Monsoons*. Toronto: Wiley, 399–464.

Shukla, J., 1987b: Long-range forecasting of monsoons. In: Fein, J. S., Stephens, P. L. (eds.) *Monsoons*. Toronto: Wiley, 523–548.

Trenberth, K., 1984: Signal versus noise in the southern oscillation. *Mon. Wea. Rev.*, **112**, 326–332.

Troup, A. J., 1965: The southern oscillation. *Quart. J. Roy. Meteor. Soc.*, **91**, 490–506.

Vernekar, A. D., Zhou, J., Shukla, J., 1994: The effect of Eurasian snow cover on the Indian monsoon. *J. Climatol.* (submitted).

Wainer, I., Webster, P. J., 1993: Monsoon-ENSO relationships in a coupled ocean-atmosphere model. *Quart. J. Roy. Meteor. Soc.*, (submitted).

Walker, G. T., 1923: Correlation in seasonal variations of weather III: A preliminary study of world weather. *Mem. Indian Meteor. Dept.*, **24**, 75–131.

Walker, G. T., 1924: Correlation in seasonal variations in weather. IV: A further study of world weather. *Mem. Indian Meteor. Dept.*, **24**, 275–332.

WCRP: World Meteorological Research Program, 1986: Scientific Plan for the Tropical Ocean Global Atmosphere Programme, WCRP Pub. #3, World Meteorological Organization, Geneva, 146 pp.

Webster, P. J., 1972: The response of the tropical atmosphere to local study forcing. *Mon. Wea. Rev.*, **100**, 518–541.

Webster, P. J., 1983: Mechanisms of monsoon low-frequency variability: Surface hydrological effects. *J. Atmos. Sci.*, **49**, 2110–2124.

Webster, P. J., 1994: The role of hydrological processes in ocean-atmosphere interaction. *Rev. Geophys*, (to appear).

Webster, P. J., Chou, L., 1982: Low frequency transitions of a simple monsoon system. *J. Atmos. Sci.*, **37**, 368–382.

Webster, P. J., Yang, S., 1992: Monsoon and ENSO: Selectively interactive systems. *Quart. J. Roy. Meteor. Soc.*, **118**, 877–926.

Webster, P. J., Chou, L., 1982: Low frequency transitions of cycle of the coupled ocean-atmosphere system of the Indian Ocean. *Quart. J. Roy. Meteor. Soc.* (submitted).

Yasunari, T., 1987: Global structure of the El Niño/Southern oscillation. Part II. Time evolution. *J. Meteor. Soc. Japan*, **65**, 81–102.

Yasunari, T., 1991: The monsoon year—a new concept of the climate year in the tropics. *Bull. Amer. Meteor. Soc.*, **72**, 1331–1338.

Zebiak, S. E., Cane, M. A., 1987: A model El Niño-Southern oscillation. *Mon. Wea. Rev.*, **115**, 2262–2278.

Author's address: P. J. Webster, Program in Atmospheric and Oceanic Sciences, University of Colorado, Campus Box 311, Boulder, Co 80309, U.S.A.